

# MICROSTRUCTURAL TEXTURE IN MATERIALS SCIENCE: REFRACTORIES

M. Velez and M. Karakus

Ceramic Engineering Dept., University of Missouri-Rolla, Rolla, MO 65409-0330 USA

[mvelez@umr.edu](mailto:mvelez@umr.edu)

## Abstract

This work summarizes important aspects of microstructure analysis of ceramics, emphasizing refractories. The objective is to use texture as a way of characterization. A comparison is made within different fields of Materials Science. The work is also part of an effort of organizing a huge database available on new and used refractories obtained from a range of applications. In this particular case, examples of applications in refractories for glass tank melters are presented. The final goal is to create a web digital library of microstructures for structural, refractory ceramic materials and related materials (i.e., stones as defects in glasses, raw materials).

**Key words:** Cathodoluminescence, Ceramic materials, Optical microscopy, refractories

## Resumen

Este trabajo presenta algunos aspectos importantes en el análisis de la microestructura de materiales cerámicos, haciendo énfasis en refractarios. El objetivo principal es la descripción de la textura como parte de la caracterización de estos materiales. También se presenta una comparación en diferentes campos de la Ciencia de Materiales. El trabajo es un paso en un esfuerzo de organizar la información disponible en relación a refractarios nuevos y usados (post mortem) en varias aplicaciones. En particular, se presentan ejemplos de refractarios empleados en la fusión y producción de materiales vítreos. La meta final es crear una biblioteca digital, disponible en Internet, sobre la microestructura de materiales cerámicos y ejemplos relacionados (i.e., defectos en vidrio provenientes de materiales refractarios, materias primas)

**Palabras Clave:** Catodoluminescencia, Cerámicas, Microscopía óptica, Refractarios

## 1. Introduction

A surface property that has a direct impact on the results of many types of analysis of materials is its texture or roughness. In general, *texture* can be defined as any three dimensional feature(s) found on a very small or large surface, and these features can range in size from the atomic level (~10 nm, as in an orderly array of atoms) to earth-size or macro level (tens of km, as in satellite imagery of the earth surface). Texture is sometimes referred in Materials Science by other terms, including *surface appearance*, *surface texture*, *surface topology*, *surface morphology*, *surface topography*, *crystallographic texture (or preferred orientation of crystallites)*, *surface roughness*, *rugosity*, *particle shape*, *spatial structure of the surface layer*, *texture of rocks (as in Geology, where sedimentary rocks are described by the size and shape of its constituents particles)*, *mathematical morphology*, and *pattern spectrum*. Selecting the right/correct/best characterization method is critical to accurately describing the exact texture of the surface in question and its features.

Examples of applications are found in the analysis of very flat surfaces, such as polished silicon wafers, and also on metals and ceramics, with roughness in the

order of micrometers. Two surface roughness terms are commonly used: average roughness, RA, and root-mean-square, RMS. For N measurements of height  $z_i$  and average height  $\bar{z}$ , the average roughness is the mean deviation of the height measurements and can be described as:

$$RA = \left( \frac{1}{N} \sum_{i=1}^N |z_i - \bar{z}| \right)$$

and RMS is the standard deviation

$$RMS = \left[ \frac{1}{N} \sum_{i=1}^N (z_i - \bar{z})^2 \right]^{1/2}$$

Several measurement techniques are in usage today, the optimum method depends on the type and scale of roughness to be measured for a particular application. *Surface roughness* is commonly measured using mechanical and optical profilers, SEM, and atomic force and scanning tunneling microscopes. In the profilometer technique, a stylus connected to an electromechanical transducer is dragged along the surface, and the centerline average (CLA) roughness is calculated from the mean amplitude of the fluctua

tions of the amplified electrical signal.

Angle-resolved scatterometers are also applied to surface roughness measurement. Depth of resolution is an important parameter for characterization (Table I). Optical scatterometry involves illuminating a sample with light and

measuring the angular distribution of light that is scattered. The technique is useful for characterizing the *topology* of two general categories of surfaces. First, on surfaces that can be defined by some surface statistics, and second, for the shapes of structures (lines) of periodically patterned surfaces.

Table 1. Analytical methods for surface characterization (adapted from [1]).

| Technique  | Depth resolution   | Lateral resolution   | Observations   |
|--|--|--|--|
| Light microscopy   | 0.2 $\mu\text{m}$ with white light                                       |  | Morphology, optical properties   |
| Optical microscopy with cathodoluminescence [2]                                | 10 nm to several $\mu\text{m}$ , depending on electron beam energy       | $\sim 1 \mu\text{m}$   | Qualitative and quantitative analysis of defects, and their distribution |
| Mechanical profiler [3]  | 0.5 nm   | 0.1-25 $\mu\text{m}$   | Measures surface roughness   |
| Optical scatterometer  | 0.1 nm   | Laser wavelength used to illuminate the sample   | Topography characterization  |
| Optical profiler   | 0.1 nm   | 0.35-9 $\mu\text{m}$   | Surface roughness  |
| SBM  | From nm to $\mu\text{m}$ , depending on the accelerating voltage         | 1-50 nm in secondary electron mode   | (images can be enhanced by using stereo pairs)                           |
| SLM <sup>a</sup> [4]   |  |  | Topography data of surface texture                                       |
| STM/SFM <sup>b</sup>   | STM, 0.1 nm;<br>SFM, 1 nm  | STM, atomic;<br>SFM, atomic to 1 nm  | Real-space 3D imaging, high resolution profilometry                      |
| TEM  | None   | 0.2 nm or better   | Atomic structure and microstructural analysis                            |
| EDS <sup>c</sup>   | 0.02 to $\mu\text{m}$  | 0.5-1 $\mu\text{m}$ for bulk samples; $\sim 1$ nm for thin sections in STEM <sup>d</sup> | Imaging/mapping of chemical elements                                     |
| STEM <sup>d</sup>  | None   | Imaging, 0.2-10 nm;<br>EELS <sup>e</sup> , 0.5-10 nm;<br>EDS <sup>c</sup> , 3-30 nm      | Microstructural, crystallographic and compositional analysis             |
| EPMA <sup>f</sup>  | 100 nm to 5 $\mu\text{m}$  | 100 nm to 5 $\mu\text{m}$  | Quantitative analysis of major, minor, and trace constituents            |
| LEED <sup>g</sup>  | 0.4-2 nm   | 0.1 mm to $\sim 10 \mu\text{m}$  | Surface crystallography and microstructure                               |
| RHEED <sup>h</sup>   | 0.2-10 nm  | 200 $\mu\text{m}$ x 4 mm   | Surface structure of crystals, distinguishes between 2D and 3D defects   |
| ESCA <sup>i</sup><br>AES <sup>j</sup><br>ISS <sup>k</sup><br>SIMS <sup>l</sup> | AES, 5-10 nm;<br>ISS, outermost atomic layer;<br>SIMS, 1 or 2 monolayers | AES, 30 nm;<br>ISS, 150 $\mu\text{m}$ ;<br>SIMS, down to 100 $\mu\text{m}$               | Surface composition characterization                                     |

<sup>a</sup>Confocal Scanning Laser Microscopy

<sup>b</sup>Scanning Tunneling Microscopy and Scanning Force Microscopy

<sup>c</sup>Energy-Dispersive X-Ray Spectroscopy

<sup>d</sup>Scanning Transmission Electron Microscopy

<sup>e</sup>Electron Energy-Loss Spectrometry

<sup>f</sup>Electron Probe X-Ray Microanalysis

<sup>g</sup>Low-Energy Electron Diffraction

<sup>h</sup>Reflection High-Energy Electron Diffraction

<sup>i</sup>Electron Spectroscopy for Chemical Analysis

<sup>j</sup>Auger Spectroscopy

<sup>k</sup>Ion Scattering Spectroscopy

<sup>l</sup>Secondary Ion Mass spectrometry

Surface damage in terms of craters, cracks, voids, and roughness has been reported in relation to machining brittle materials, such as ceramics. Except perhaps for the intent of quantitatively describing irregular fracture surfaces with *fractal geometry* [5], most of this work is based on descriptive observations from micrographs (optical or electron microscopy) with little quantifying of the damage. Surface damage will effect deterioration of the mechanical properties, such as strength. In order to characterize the surface integrity of machined surfaces of ceramics, the flexural strength can be used as measurement since it is dependent on both its inherent resistance to fracture and the presence of defects [6]. Applications are found, for instance, in the characterization of limestone calcined under different conditions [7].

The surfaces of most particles are rough on a microscopic scale, and the contact occurs at high points, which are called asperites [8]. Layer silicate minerals and pristine amorphous solids have relatively smooth surfaces with irregularities finer than 100 nm. Crushed minerals have surfaces with step-like features coarser than a few microns, and aggregates have very rough surfaces with irregularities approaching the crystallite size. Interparticle friction and sliding is resisted by chemical adhesion and physical resistance produced by the microscopic steps and asperites on the particle surfaces.

*Pattern Recognition Theory* has been introduced to perform *surface textures* classification [9], and in general to describe better the texture of *engineering surfaces* using computer and mathematical tools. For instance, using Atomic Force Microscopy (AFM) image representing the surface textures of various materials formed by various processes and treated by mathematical transformations. The results are linked to properties of surface materials and the process of growth and crystallization on the interface of different materials. Other advanced techniques are represented by the attainment of *fractal dimensions* from SEM images [10], the use of Scanning Tunneling Microscopy (STM) to characterize mathematically surface texture parameters [11], the analysis of fiber optic transducer and conventional profilometer data by use of statistical functions [3], and by using Fourier analysis of AFM images [12]. Another emerging techniques include *Gaussian Texture Analysis* of SEM micrographs, as in this case, of organic materials, carried by the Center of Imaging Science [13]. In particular, the work at the Center of Imaging Science at Rochester University on morphological texture classification indicates that gray-scale *granulometric classifiers* can discriminate between textures that have rather similar visual characteristics [14].

This work exemplifies different microstructure textures encountered in Ceramics, with special emphasis in refrac-

tories using optical and electron microscopy. Several examples are typified and some problems are presented.

## 2. Texture in Materials

### 2.1. Ceramics

Orienting or aligning a second phase such as fibers, whiskers, and platelets during green body or powder consolidation processing can achieve textured ceramics. Textured ceramics show improved or unique properties (electrical, magnetic, and mechanical, for instance) and have been obtained by applying field gradients during fabrication. *Texture* can be developed in ceramics, which lack plasticity as compared to metals, by grain rotation or oriented anisotropic grain growth [15]. Common processing methods include hot-forging, hot-pressing, tape casting, extrusion, and slip casting. As an example, high-textured mullite has been obtained by enhancing the anisotropic grain growth by TiO<sub>2</sub>-doping and by templating grain growth on oriented acicular mullite seed particles in a mullite precursor [16]. The in situ grain growth and alignment was developed by tape casting in mullite-whisker-seeded and titania-doped diphasic mullite gels.

Processing also has effect on the crystallographic texture domain, as on the successive thermomechanical treatment of Bi-based (2223) superconductor Ag-sheated tapes, by pressing and rolling results indicate a large increase in the crystalline density and preferred orientation in the initial steps, and saturation after the third cycle of treatment [17]. Another applications are found on eteroepitaxial diamond film growth [18], humidity-sensing behavior of sulfated zirconia [19], surface texture of multicrystalline silicon solar cells [20], and the fabrication and evaluation of composite ionic conductors [21].

### 2.2 Comparison to Metals

Local variations in chemical composition and microstructure arise during manufacture and processing of metals. Furthermore, the microstructure might be anisotropic, and variations might exist, for example, between the transverse and the longitudinal direction of rolled metal bars or *textures* may occur. Textured surfaces can be used to impart a number of desirable properties or characteristics on finished metal products [22]. The types of textures that are often rolled onto the sheets used for refrigerator panels serve to conceal dirt, for instance. Embossed or coined protrusions can enhance the grip of metal stair treads and walkways. Corrugations provide enhanced strength and rigidity. Still other textures can be used to modify the optical or acoustical characteristic of a material.

*Crystallographic Texture* develops in metals during plastic deformation by slip plane rotation. *Preferred orientation* in polycrystalline materials can be detected with a Debye-Scherrer camera and diffractometer with texture attachment [23].

The use of electron backscattering diffraction patterns (EBSPs) in conjunction with SEM allows the determination of *preferred orientation*, or *crystallographic texture*, in combination with microstructural data [24]. Examples are found in textures induced by extrusion of aluminum alloys [25, 26], processing of zinc electrogalvanized coatings [27], electrodeposition of polycrystalline Ni [28], processing of ferritic alloys [29] and steels [30].

The analysis of microstructural images (Quantitative Metallography) can be considered as an abstract problem of 2D or 3D geometry without any account of the actual phase compositions. This branch is termed *Mathematical Morphology* (MM) and it is generally valid for all microstructures [31]. The methods of MM are designed to quantify geometric structures; a porous medium, for instance, is made of two complimentary sets, grains and pores. Quantifying any structure then comes down to measuring sets, obtained by successive transformations, which from the initial image will progressively reveal the set to be measured. These transformations are combinations of elementary morphological transformations [32].

Quantitative metallography refers to the accumulation of data necessary to describe a 3D microstructure, that is, its 3D dimensional geometry, usually to correlate microstructure to manufacturing or performance history. The geometric parameters are described based on the standard morphological, such as maximum particle diameter or mean intercept length. The following possibilities for quantifying the microstructure are available [31]:

1. Description of basic 2D parameters such as area fraction, and planar size distribution;
2. Complex 2D description including shape and arrangement of mathematical morphology;
3. 3D description by stereological parameters such as volume fraction, spatial size distribution, specific surface area, derived from 2D measurements; and
4. Direct evaluation of 3D geometry by sectioning or stereometric measurements.

### 2.3 Catalysts and Ceramic Membranes

Textural properties of catalysts are an important area of characterization of catalytic materials. It comprises surface area, total pore volume, and mean pore radius [i.e., 33, 34] and texture. Surface area, pore size and pore volume are among the most fundamental and important prop-

erties in catalysis because the active sites are present or dispersed throughout the internal surface through the reactants and products are transported. The size and number of pores determine the internal surface area. It is usually advantageous to have high surface area (high density of small pores) to maximize the dispersion of catalytic components; however, large molecules might be excluded from passing through the small pores, which might have an important effect in given process. The pore structure and surface area must be optimized to provide maximum utilization of active catalytic sites for a given feedstock [35]. A pure metal catalyst will change in *surface roughness* or crystal structure during use.

Promoters in catalysis can be classified as either *textural promoters* or structural promoters. A textural promoter is an inert substance, which inhibits the sintering of microcrystals of the active catalyst, by being present in the form of very fine particles (physical effect), while structural promoters act by a chemical effect. As example of application, chromia/zirconia catalysts have been tailored in texture from micro porous to mesoporous and macroporous materials [36].

*Crystallographic texture* is also of interest in the development of special functions in membranes, for instance, special boehmite gel membranes exhibit (020) texture, and the (020) surface of gamma-AlOOH (boehmite) grains are parallel to the top surface of the membrane [37].

### 2.4 Cement Pastes and Concrete

The morphological characteristics of coarse aggregates can be measured by standard methods such as the test method for *index and particle shape and texture* (ASTM D- 3398); the test method for uncompact void content of coarse aggregate as influenced by *particle shape, surface texture, and grading* (ASTM C-1252); and the test method for unit weight and voids in aggregate test (ASTM C-29). Digital Image-analysis has also been used to characterize coarse aggregates, by using improved techniques as in evaluating asphalt-concrete mixtures [38].

The particle shape and surface texture of normal Portland cement and supplementary materials has been observed by using AFM where neither profilometer [39] nor SEM [40] can provide detailed images of the fine materials. It has been shown for example, that silica fume is composed of two complimentary parts (hemispheres or cylinders), nano-size particles are found in all materials, and a relatively smooth surface was observed in the hydrated cement paste [41]. *Fine texture* is referred as a general indication of grain size, as in the measurement of alite grains using polished cross sections in Portland cement clinker [42], measured by optical microscopy.

Computational research on cement-based materials, directly related to microstructure development, is a current area of work. Cement-based materials are considered random composites over many length scales and understanding of the

macro- and microstructure would lead to the understanding of the microstructure-property relationships [43]. For instance, one current approach at the National Institute of Standard Materials (NIST) is to characterize the microstructure of concretes using optical and electron microscopy and digitizing the information (color, texture, and geometrical parameters). The digital data is then analyzed and used to simulate hydration reactions, percolation problems, and microstructure development.

## 2.5 Refractories

The phase composition, porosity, and *texture* of refractories are determined experimentally, routinely using at least optical and electron microscopy of polished samples. The starting compositions, and particle sizings, and processing techniques together with firing schedule, affect the results. Thus, crystallite size and aggregate size are a measure of texture in refractories, defects such as microcracks can also be imaged and measured. In many refractory bricks, pre-existing cracks are in the millimeter range, even up to the order of 10 mm. An increasing extent of microcracking must accompany increasingly coarse-crystalline microstructures and the use of still coarser-sized premanufactured grain or aggregate is common [44]. Accordingly, depending on the *coarseness of their texture*, refractories can be expected to have a markedly below-ceramic Young's modulus values. A further consequence of micro cracking with open porosity, which also sets refractories apart from fine-grained ceramics, is a sharp reduction of the elastic limit. Texture and coarseness also have influence on corrosion behavior of refractories. Since the surface:volume ratio of the grain particles increases as their size decreases, the smaller particles are successively more vulnerable to corrosive-liquid attack. Thus, compromising the corrosion resistance of the grain somewhat by the use of graded sizing improves the resistance of the grain-matrix-pore system as a whole.

Physical characterization of refractory aggregates routinely include visual analysis (macro- and microscopic), particle size distribution, packing density, aggregate shape, *surface texture*, and particle density — where surface texture indicates the 2D rendering of the surface, or perhaps the 3D detailing of the physical surface; i.e., *surface morphology*. Microcracking and presence of inclusions can also be noted by visual analysis and description of the surface texture.

Most monolithic refractories contain alumina aggregates of various types including fused aluminas, tabular alumina, and calcined bauxite. The surface morphology is enhanced by using special techniques, such as optical microscopy assisted with cathodoluminescence (CLM) of polished sections. The analysis of different refractories using CLM has been presented earlier [45-48]. Thermal annealing of high-

alumina ceramics coupled with scanning electron microscopy is another commonly employed method.

## 2.6 Post-mortem Study of Glass Melting Furnace Refractories

The Refractories Research Center in University of Missouri-Rolla initiated the research program "Post-mortem characterization of glass plant refractories", in 1996, in order to understand refractory corrosion mechanisms and to develop refractories for the glass making industry. The program involves collection of a large group of post-mortem glass plant refractories and their characterization as well as laboratory corrosion test simulation. Cathodoluminescence Microscopy (CLM) technique is the primary characterization technique. The description and advantages of the technique and the preliminary study of the post-mortem glass plant refractories have already been summarized [49].

Figures 1 and 2 show the corrosion texture of silica refractories [50] under optical and electron microscopy. Reflected light (Fig. 1a) shows the typical "fish scale" morphology of cristobalite, however, CLM shows the dendritic morphology that indicates a liquid phase (about 250  $\mu\text{m}$  thick) during refractory service. It also shows cristobalite at deeper locations, as well as prismatic tridymite, and wollastonite green fibers.

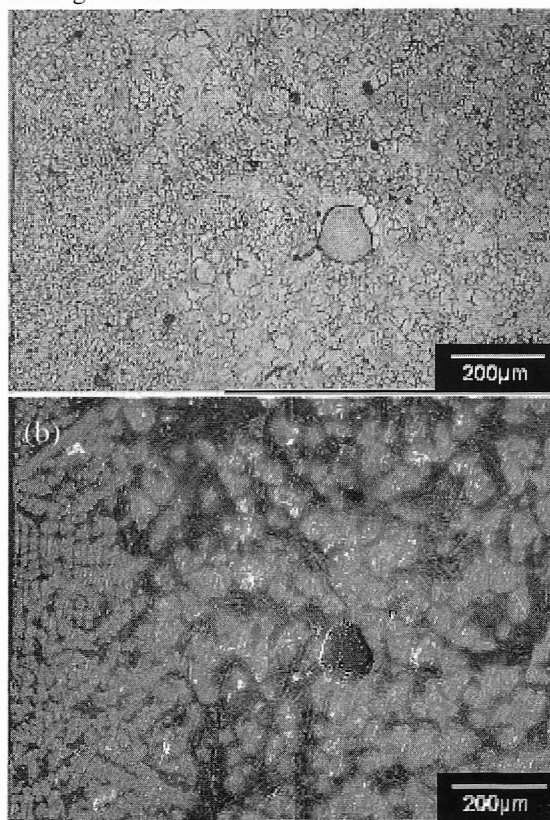


Fig. 1. Optical microscopy (reflected light and cathodoluminescence) of a silica crown brick exposed to oxyfuel conditions. Dendrite crystals of cristobalite (blue CL) and amorphous  $\text{Na}_2\text{O}$ -rich Ca-silicate glass matrix are shown at the hot face (left side).

A similar information is obtained using SEM (Fig. 2), however, this technique is more expensive than CLM. Both techniques are complementary and for complete analysis chemical analysis (wet method of core sections), SEM probe analysis, and XRD is routinely made. Corrosion of AZS checker bricks by alkalis and alkali sulfates has also been studied and described earlier [51].

Another application is the study of microstructures of regenerator bricks in glass tank melters. Figure 3 illustrates the microstructure of a periclase checker brick containing 95-98 % MgO. The material had a visual shattered or burst appearance. The interior of the brick was pink in color while the outer surface was green in color. Under the optical microscope, periclase grains exhibited red CL color. Also, silicate phases forsterite and monticellite were identified. Grain growth of periclase in the outer burst surface was also noted. Thermal fluctuation, volume reduction, grain growth, and silicate phase formation are the causes for the failure (bursting) of these checker bricks.

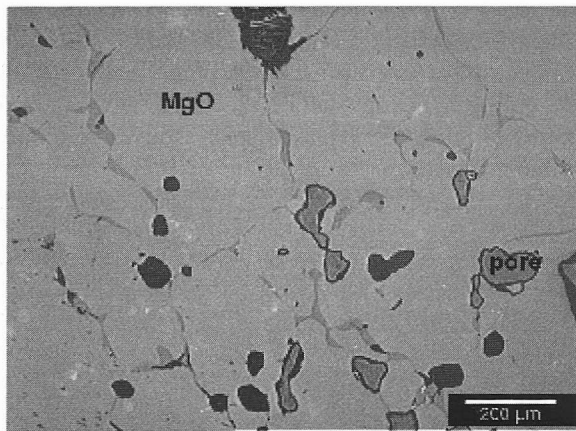


Fig. 2. SEM micrograph of a commercial silica crown brick exposed to oxyfuel conditions (1500°C, 200-300 ppm NaOH, 10 days). Hot face is at left side, a few closed pores remain usually larger than 400-500 microns.

Fig. 3. RL and CL micrographs of 98 % periclase checker brick from top course showing grain growth of periclase. Many pores are entrapped and enclosed within the periclase grains which are visible in the CL micrograph. Monticellite (yellow CL) is observed at the grain boundaries of periclase

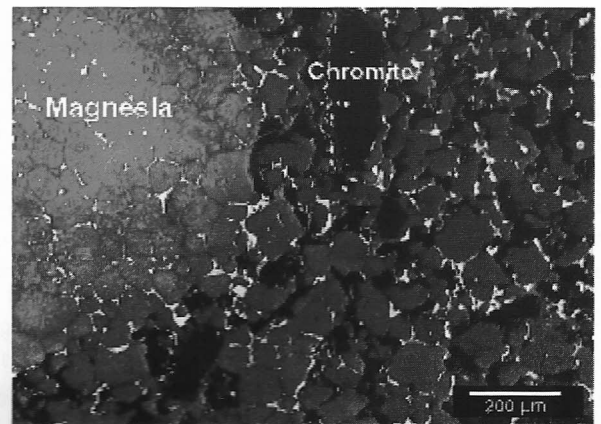
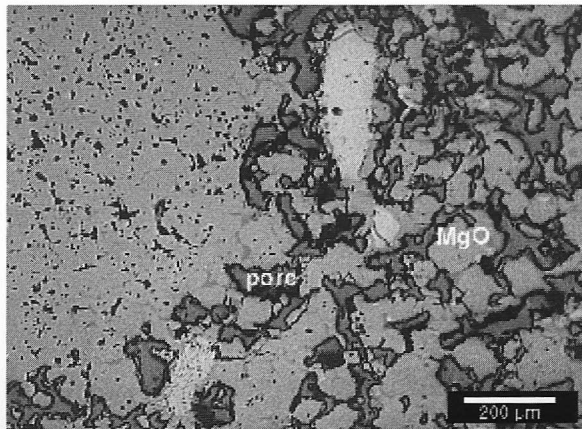


Fig. 4. RL and CL micrographs of direct bonded Mag-Chrome checker brick, showing a silicate impurity phase, primarily monticellite (yellow CL) at grain boundaries.

Figure 4 illustrates the microstructure of direct-bonded Mag-Chrome regenerator crown bricks. The surface of these bricks was damaged and extremely crumbly. In this zone, high porosity, silicate impurities as well as sulfate phases were observed. Although these bricks were direct-bonded, they still contain significant amounts of silicate phases.

The last example (Fig. 5) illustrates the microstructures of chrome-free, fused cast, cruciform AZS block. This sample was 2 inches thick and was coated with a yellowish foam-like glassy material. It had a crumbly appearance and broke in a columnar habit. The original material was known to be a fused cast, chrome free, AZS checker brick with a chemistry of 50.6 %  $\text{Al}_2\text{O}_3$ , 32.5 %  $\text{ZrO}_2$ , 15.6 %  $\text{SiO}_2$ , and 1.3 %  $\text{Na}_2\text{O}$ . The foam-like coating on the surface contained Na-Ca-sulfate,  $\text{Na}_2\text{Ca}(\text{SO}_4)_2$ , Na-Ca-Mg-Al-silicate phase, spinel, zircon and other dust particles. It is

very clear that the checker bricks were subjected to a very corrosive gaseous and dust environment. The original material did not contain any CaO, MgO, and S. The alkaline sulfates and dusts from the batch carry over react with the checker brick resulting in foamy surface texture due to the glass formation and volume changes.

An ultimate goal of the characterization program at UMR is the creation of a digital library for refractories, including refractories for glass manufacturing, defects in glasses and raw materials. Several independent techniques can be summarized into a large database that can provide easy access and full documentation to users (students, field engineers, technicians, researchers). This could result in a unified source of information for ceramic microstructures, regarding definitions, norms, and specific terminology.

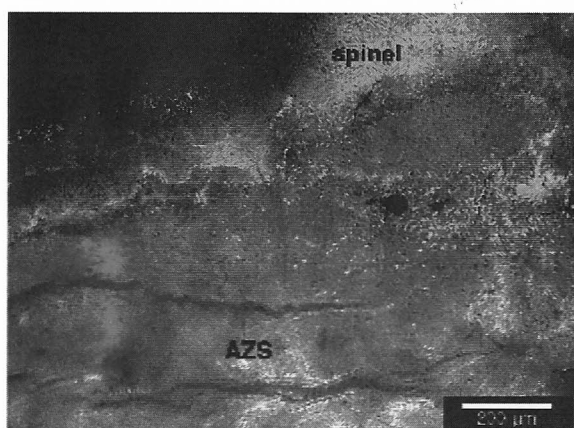
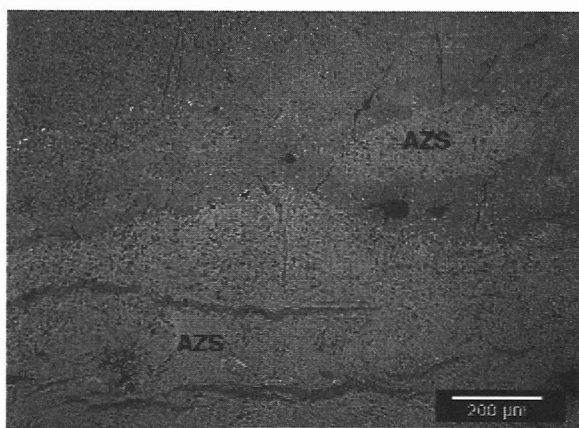


Fig. 5. RL and CL micrograph of fused-cast, chrome-free cruciform AZS checker brick showing corrosion and peeling-off AZS material by alkalis and alkaline earth sulfates. Spinel (green CL),  $\text{Na}_2\text{Ca}(\text{SO}_4)_2$ , as well as Na-Ca-Mg-Al-silicate phases were formed as results of reaction between alkaline sulfates and AZS checker brick.

### 3. Conclusions

This work summarizes important aspects of microstructure analysis of ceramics, emphasizing refractories. The objective is to use texture as a way of characterization. A comparison is made within different fields of Materials Science. Characterization of materials is important to decide on the performance under different conditions (microstructure-properties relationship and prediction of properties, failure analysis, product development) and depends on the use of several techniques. The identification routinely consists on the confocal use of various methods: chemical analysis, X-ray diffraction, physical and chemical properties determination, etc., with the use of agreed norms and regulations (i.e., ASTM standards, DIN, etc.). One common technique of identification is the use of opti-

cal and electron microscopy. Such work describes the morphology of the materials at different resolution levels. Cathodoluminescence microscopy (CLM) examples are presented here as an alternative for a supplemental technique to aid in the identification and characterization of refractories. The technique is suitable for most cases whereas most powerful techniques, such as SEM, may add very little in some cases and/or are more expensive. CLM (color images), and all microscopy in general, present the information in image data form. This makes mandatory the use of an electronic version for the digital display of the information. The final objective of the program at UMR is to create a digital library of ceramic microstructures (DLCM) for structural, refractory materials and related cases.

## References

1. C. R. Brundle, C. A. Evans, S. Wilson, "Encyclopedia of Materials Characterization," p. 53, Materials Characterization Series, Butterworth-Heinemann, 1992.
2. M. Karakus, R. E. Moore, "Characterization of Aggregates and Other Starting materials for Monolithic Refractories," 35th Annual Symposium on Refractories, The St. Louis Section of the American Ceramic Society, March 26, 1999.
3. W. Scott, A. Donovan, "Comparison of Surface Texture Measurement by Stylus and Fiber Optic Transducers," *J. of Testing & Evaluation*, [26] 70-78 (1998).
4. S. Hara, K. Yanagi, S. Matsuo, R. Yamada, "Surface Topography Measurement Using Confocal Scanning Laser Microscopy and Functional Digital Filtering," *J. of the Japan Society of Precision Engineering*, 64[5] 710-714 (1998).
5. J. J. Mecholsky, S. W. Freiman, "Relationship Between Fractal Geometry and Fractography," *J. Am. Ceram. Soc.*, 74[12] 3136-3138 (1991).
6. T. C. Lee, J. H. Zhang, Y. K. Lok, "Surface Modification of Wire Electro-Discharge Machined Sialon Ceramics by Ultrasonic Finishing," pp. 411-417, in Ceramic Material Systems with Composite Structures. Towards Optimum Interface Control and Design, N. Takeda, L. M. Sheppard, J-I. Kon (editors), Ceram. Trans. Vol. 99, The American Ceramic Society, 1998.
7. K. Wiczorek-Ciurawa, "Peculiarities of Interaction in the CaCO<sub>3</sub>/CaO-SO<sub>2</sub>/SO<sub>3</sub>-Air System. A Review," *J. Thermal Analysis*, 53[2] 649-658 (1998).
8. J. S. Reed, "Introduction to the Principles of Ceramic Processing," pp. 205, Chapter 14, John Wiley, 1988.
9. A. Ya. Grigoriev, S. A. Chizhik, N. K. Myshkin, "Texture Classification of Engineering Surfaces with Nanoscale Roughness," *International J. of Machine Tools & Manufacture*, 38(5-6) 719-724 (1998).
10. R. D. Bonetto, J. L. Ladaga, "Variogram Method for Characterization of Scanning Electron Microscopy Images," *Scanning*, 20[6] 457-463 (1998).
11. M. Aguilar, A. I. Oliva, E. Anguiano, "Importance of Imaging in Scanning Tunneling Microscopy for the Determination of Surface Texture and Roughness," *Surface Sci.*, 420[2-3] 275-284 (1999).
12. K. Carneiro, C. P. Jensen, J. F. Jorgensen, J. Garnoes, P. A. McKeown, "Roughness Parameters of Surfaces by Atomic Force Microscopy," *Cirp Annals*, 44(I) 517-522 (1995).
13. Consortium which includes John Hopkins University, Harvard, MIT Lincoln Laboratory, and the University of Texas at Austin.
14. Y. Chen, E. R. Dougherty, "Gray-Scale Morphological Granulometric Texture Classification," *Optical Eng.*, 33[8] 2713-2722 (1994).
15. M. S. Sandlin, K. J. Bowman, "Textures in AlN-SiC Composite Ceramics," pp. 263-268 in Materials Research Society Symposium Proceedings, Vol. 327, Covalent Ceramics II, Non-Oxides, Materials Research Society, 1994.
16. S-H. Hong, G. L. Messing, "Development of Textured Mullite by Templated Grain Growth," *J. Am. Ceram. Soc.*, 82[4] 867-872 (1999).
17. P. A. Suzuki, M.C.A. Fantini, "Investigations on the Texture of Bi-Based Superconductor Tapes," *Mat. Sci. & Eng. B*, I, 1-9 (1994).
18. J. Mossbrucker, W. S. Huang, B. Wright, V. Ayres, S. Khatami, J. Asmussen, "Investigation in the Effect of Nitrogen Incorporation in Heteroepitaxial Diamond Film Growth, Texture, Morphology, and Crystalline Quality," pp. 222 4P49, in *IEEE International Conference on Plasma Science Proc.*, 1998.
19. I. S. Mulla, S. D. Pradhan, K. Vijayamohan, "Humidity-Sensing Behaviour of Surface-Modified Zirconia," *Sensors & Actuators A*, 57[3] 217-221 (1996).
20. I. S. Mulla, S. D. Pradhan, K. Vijayamohan, "Humidity-Sensing Behaviour of Surface-Modified Zirconia," *Sensors & Actuators A*, 57[3] 217-221 (1996).
21. M. Nagai, T. Nishino, "Fabrication and Evaluation of Composite Ionic Conductors by the Use of a Temperature and Concentration Gradient," *J. Mat Synthesis & Processing*, 6[3] 197-201 (1998).
22. E. P. DeGarmo, J. T. Black, R. A. Kohser, "Materials and Processes in Manufacturing, 8th edition, pp.1109, Prentice Hall, 1997.
23. J. B. Watchman, Z. H. Kalm, Characterization of Materials, p. 323, Butterworth-Heinemann, 1993.
24. S. Amelinckx, D. van Dyck, J. van Landuyt, G. van Tendeloo (editors), p. 124 in Handbook of Microscopy, Applications in Materials Science, Solid-State Physics and Chemistry, Weinheim, 1997.
25. A. Poudens, B. Bacroix, T. Brelheau, "Influence of Microstructures and Particle Concentrations on the Development of Extrusion Textures in Metal Matrix Composites," *Mat. Sci. & Eng. A*, 1-2,219-228 (1995).
26. K. Karhausen, A. L. Dons, T. Aukrust, "Microstructure Control During Extrusion with Respect to Surface Quality," *Mat. Sci. Forum*, 217-222[1] 403-408 (1996).
27. H. Park, J. A. Szpunar, "Role of Texture and Morphology in Optimizing the corrosion Resistance of Zinc-Based Electrogalvanized Coatings," *Corrosion Sci.*, 40[4-5] 525-545 (1998).
28. F. Czerwinski, G. Palumbo, J. A. Szpunar, "Textures of Oxide Films Grown on Nickel Electrodeposits," *Scripta Materialia*, 39[10] 1359-1364 (1998).

29. A. Alamo, H. Regle, J. L. Bechade, "Effects of Processing Textures and Tensile Properties of Oxide Dispersion Strengthened Ferritic Alloys Obtained by Mechanical Alloying," pp. 169-182 in Powder Processing Advances in Powder Metallurgy, Metal Powder Industries Federation, Princeton, Vol. 7, 1996.
30. J. Mizera, A. Garbacz, K. J. Kurzydowski, "Texture Evolution during Tensile Deformation of an Austenitic Steel and its Effect on the Distribution of CSL Boundaries," *Scripta Metallurgica et Materialia*, 33[4] 515-519 (1995).
31. H. E. Exner, H. P. Hougardy, (editors) "Quantitative Image Analysis of Microstructures," DGM Informationsgesellschaft, 1988.
32. S. Beucher, "Micromorph, A Mathematical Morphology Tutorial Software," Centre de Morphologie Mathematique, Ecole des Mines de Paris, www.cmm.ensrnp.fr/Micromorph/
33. T. Elnabarawy, A. A. Attia, M. N. Alaya, "Effect of Thermal Treatment on the Structural Texture and Catalytic Properties of the ZnO-Al<sub>2</sub>O<sub>3</sub> System," *Materials Letters*, 24[5] 319-325, 1995
34. L. R. Mentasty, O. F. Gorriz, L. E. Cadus, "Chromium Oxide Supported on Different Alumina Supports: Catalytic Propane Dehydrogenation," *Ind. Eng. Chem. Res.*, 38, 396-404 (1999).
35. R. J. Farrauto, M. C. Hobson, "Catalyst Characterization," pp. 563-589, in Encyclopedia of Physical Science and Technology, Vol. 2, The Academic Press, Inc., 1987.
36. A. Cimino, D. Cordischi, S. De Rossi, G. Ferraris, D. Gazzoli, V. Indovina, G. Minelli, M. Occhiuzzi, M. Valigi, "Studies on Chromia/Zirconia Catalysts, I. Preparation and Characterization of the System," *J. Catal.*, 127, 744-760 (1991).
37. X. Huang, Z. Huang, "Textured Growth of Boehmite Gel Membranes," *J. Chinese Ceram. Soc.* 25[1], 110-114(1997).
38. Ch-Y. Kuo, R.S. Rollings, L. N. Lynch, "Morphological Study of Coarse Aggregates Using Image Analysis," *J. Mat. Civil Eng.*, 10[3] 135-142 (1998).
39. W. A. Tasong, C. J. Lynsdale, J. C. Cripps, "Aggregate-Cement Paste Interface. II Influence of Aggregate Physical Properties," *Cement & Concrete Res.*, 28[10] 1453-1465 (1998).
40. K. E. Wagner, E. A. Draper, J. Skalny, "Use of Complementary Imaging Techniques in Concrete Deterioration Studies," *MRS Bulletin*, 18[3] 60-65, 1993.
41. V. G. Papadakis, E. J. Pedersen, H. Lindgreen, "AFM-SEM Investigation of the Effect of Silica Fume and Fly Ash on Cement Paste Microstructure," *J. Mat. Sci.*, 34[4] 683-690 (1999).
42. M. Ichikawa, M. Kanaya, "Effects of Minor Components and Heating Rates on the Fine Textures of Alite in Portland Cement Clinker," *Cement and Concrete Res.*, 27[7] 1123-1129 (1997).
43. E. J. Garboczi, D. P. Bentz, "Computational Materials Science of Cement-Based Materials," *MRS Bulletin*, 18[3] 50-54, 1993.
44. S. C. Carniglia, G. L. Barna, "Handbook of Industrial Refractories Technology. Principles, Types, Properties and Applications," pp. 424, Noyes Publications, 1992.
45. M. D. Crites, M. Karakus, M. E. Schlesinger, M. A. Sommerville, S. Sun, "Interaction of Chrome-free Refractories with Copper Smelting and Converting Slags", *Canadian Metallurgical Quarterly*, 39[2] 129-134 (2000).
46. M. D. Crites, M. Karakus, M. E. Schlesinger, M. A. Sommerville, S. Sun, Refractory Interactions with Calcium Ferrite Slags, *Interceram*, 46[2] 88-91 2000.
47. A. A. Wereszczak, H. Wang, M. Karakus, W. Curtis, "Postmortem Analyses of Salvaged Conventional Silica Bricks from Glass Production Furnaces", *Glass Science and Technology, Glasstechnische Berichte*, 73[ 6] 165-174 (2000).
48. M. Karakus, J. D. Smith, R. E. Moore, "Cathodoluminescence Mineralogy of the Used MgO-C Bricks in Basic Oxygen Furnaces", *Veithsch-Radex Rundschau*, 1, 24-32 (2000).
49. M. Karakus, R.E. Moore, "Post-Mortem Study of glass Plant Furnace Refractories, in Corrosion of Materials by Molten Glass, G. A. Pecoraro, J. C. Marra, J. T. Wenzel (Eds.), pp. 179-191, Ceramic Transactions, Vol. 78, The American Ceramic Society, Westerville, OH, 1996.
50. M. Velez, J. M. Almanza, M. Karakus, "Relationship between Microstructure and Corrosion Performance of Crown Silica Bricks under Oxyfuel Combustion," submitted to *The Am. Ceram. Soc. Bull.*, 2001.
51. M. Karakus, R. E. Moore, "Seeking Solution to Glass Defects from Refractory Corrosion, *The Glass Researcher, Bulletin of Glass Science and Engineering*, 7[2] pp. 13, 14, 17 (1998).